

Exploiting Interkingdom Interactions for Development of Small-Molecule Inhibitors of *Candida albicans* Biofilm Formation

F. Jerry Reen,^a John P. Phelan,^a Lorna Gallagher,^a David F. Woods,^a Rachel M. Shanahan,^b Rafael Cano,^b Eoin Ó Muimhneacháin,^b Gerard P. McGlacken,^b Fergal O’Gara^{a,c}

Biomerit Research Centre, School of Microbiology, University College Cork—National University of Ireland, Cork, Ireland^a; School of Chemistry and Analytical and Biological Chemistry Research Facility (ABCRF), University College Cork—National University of Ireland, Cork, Ireland^b; School of Biomedical Sciences, Curtin Health Innovation Research Institute, Curtin University, Perth, Australia^c

A rapid decline in the development of new antimicrobial therapeutics has coincided with the emergence of new and more aggressive multidrug-resistant pathogens. Pathogens are protected from antibiotic activity by their ability to enter an aggregative biofilm state. Therefore, disrupting this process in pathogens is a key strategy for the development of next-generation antimicrobials. Here, we present a suite of compounds, based on the *Pseudomonas aeruginosa* 2-heptyl-4(1H)-quinolone (HHQ) core quinolone interkingdom signal structure, that exhibit noncytotoxic antibiofilm activity toward the fungal pathogen *Candida albicans*. In addition to providing new insights into what is a clinically important bacterium–fungus interaction, the capacity to modularize the functionality of the quinolone signals is an important advance in harnessing the therapeutic potential of signaling molecules in general. This provides a platform for the development of potent next-generation small-molecule therapeutics targeting clinically relevant fungal pathogens.

With the ever-increasing emergence of antibiotic-resistant pathogens and the lack of new antibiotics coming to market, we are entering a “postantibiotic era” (1–3). This realization has underpinned a global initiative to identify new and innovative approaches to infection management. As such, targeting virulence as a potential strategy for developing new antimicrobial drugs has been the focus of several research initiatives (4–11). In principle, suppressing virulence behavior and locking pathogens in a vegetative non-biofilm-forming lifestyle renders them less infective and more susceptible to conventional antibiotics (4, 12). While some success has been achieved against bacterial pathogens (6, 10, 13–19), less focus has been placed on fungal infections, which nevertheless continue to cause serious complications and mortality in patients (8, 20–22). Indeed, despite the medical and economic damage caused by fungal biofilms, there remains an urgent and largely unmet need for the identification of compounds able to specifically and selectively target and inhibit this mode of growth in clinically relevant fungal pathogens (23).

The predominant nosocomial fungal pathogens, which include *Candida* spp., *Aspergillus* spp., and *Fusarium* spp., are difficult to diagnose and cause high morbidity and mortality, even following antifungal therapy (21). *Candida albicans* causes a variety of complications ranging from mucosal disease to deep-seated mycoses, particularly in immunocompromised individuals (21, 24). Along with other fungal and yeast pathogens, *C. albicans* is known to form structured communities called biofilms on medical devices either pre- or postimplantation, leading to recurring infections and in some cases death (25, 26). Once established in the biofilm phase, *C. albicans* presents a significant clinical problem, with current treatment options severely limited by the intrinsic tolerance of fungal biofilms for antimycotics (20, 27, 28). Recent combination therapies incorporating antibacterial and antifungal agents have shown some success (29). However, as with all antibiotic-based strategies, reports of resistance continue to emerge (27), and biofilms themselves are considered a breeding ground for the emergence of antibiotic-resistant strains, effec-

tively hastening the onset of the perfect storm where the rapid decline in new antibiotic production has been met by an equally rapid increase in multidrug-resistant organisms (1). Thus, there is a need to consider new anti-infective strategies that do not target essential processes in the target organism. While blocking biofilms in these organisms remains a major clinical challenge (26, 30), exploiting our increased understanding of microbial signaling networks to control virulence and biofilm behavior is one innovative approach with significant potential.

Many sites of infection are colonized by communities of mixed fungal and bacterial organisms, and several layers of communication significantly impact the dynamics and flux of these populations (31, 32). For example, *C. albicans* is known to coexist with *Pseudomonas aeruginosa* in the cystic fibrosis (CF) lung, and interkingdom communication between the two organisms has previously been reported (16, 33). The *Pseudomonas* quinolone signal (PQS), 2-heptyl-3-hydroxy-4-quinolone, and its biological precursor, 2-heptyl-4-quinolone (HHQ), are important virulence factors produced by *P. aeruginosa*. Structurally, PQS and HHQ differ by the presence of a hydrogen at C-3 in HHQ and a hydroxyl group in PQS, giving rise to the increased interest in modulating

Received 22 January 2016 Returned for modification 21 April 2016

Accepted 1 July 2016

Accepted manuscript posted online 25 July 2016

Citation Reen FJ, Phelan JP, Gallagher L, Woods DF, Shanahan RM, Cano R, Ó Muimhneacháin E, McGlacken GP, O’Gara F. 2016. Exploiting interkingdom interactions for development of small-molecule inhibitors of *Candida albicans* biofilm formation. *Antimicrob Agents Chemother* 60:5894–5905. doi:10.1128/AAC.00190-16.

Address correspondence to Fergal O’Gara, f.ogara@ucc.ie.

F.J.R. and J.P.P. contributed equally to this work.

Supplemental material for this article may be found at <http://dx.doi.org/10.1128/AAC.00190-16>.

Copyright © 2016, American Society for Microbiology. All Rights Reserved.

this position to assign biological function to the structures of the molecules (34–37). Previously, we have shown that HHQ, but not PQS, suppresses biofilm formation by *C. albicans* (10). In response, *C. albicans* produces farnesol, which has been shown to modulate PQS production in *P. aeruginosa* (33). As both PQS and HHQ promote virulence and pathogenicity of *P. aeruginosa* (38, 39), their utility as an anti-*Candida* treatment falls short of being a viable antifungal treatment. However, the amenability of these small molecules to chemical modification provides an opportunity to develop compounds with specificity of function.

The transcriptional data and microscopic imaging described in this study have implicated components of the cell wall as key factors in the response of *C. albicans* to *P. aeruginosa* alkylhydroxyquinolone (AHQ) signaling. Furthermore, the biological activity of each class of analogue in bacterial, fungal, and host systems provides new insight into the possible interkingdom role of AHQs, particularly in a clinical setting such as the CF lung, where all three systems coexist. From a translational perspective, lead HHQ analogues with four key features were identified: (i) they have potent antibiofilm activity toward *C. albicans*, (ii) they have selective noncytotoxicity toward mammalian cell lines, (iii) they are nonagonistic and (iv) they are potentially antagonistic to the virulent pathogen *P. aeruginosa*. Several analogues retained the significant potency of the parent HHQ molecule against *C. albicans* biofilm formation while simultaneously becoming inactive in *P. aeruginosa* quorum sensing. This suggests that these molecules have the potential to be further optimized for use as anti-infectives for *Candida* without the concomitant limitation of *P. aeruginosa* virulence augmentation.

MATERIALS AND METHODS

***C. albicans* stock maintenance and culturing conditions.** *C. albicans* strain SC5314 was subcultured from 15% (vol/vol) glycerol stocks at -80°C onto yeast-peptone-dextrose (YPD) medium (1% [wt/vol] yeast extract, 2% [wt/vol] peptone, and 2% [wt/vol] dextrose) and incubated at 30°C overnight.

***P. aeruginosa* stock maintenance and culturing conditions.** *P. aeruginosa* strains, PAO1 and a *pqsA* mutant, containing the chromosomally inserted *pqsA-lacZ* promoter fusion on plasmid pUC18-mini-Tn7, were maintained on Luria-Bertani (LB) agar plates supplemented with carbenicillin (200 $\mu\text{g/ml}$) and 5-bromo-4-chloro-3-indolyl- β -D-galactopyranoside (X-Gal) (40 $\mu\text{g/ml}$) and incubated at 37°C overnight. Single colonies were inoculated into LB broth (20 ml) supplemented with carbenicillin (200 $\mu\text{g/ml}$) and incubated at 37°C with shaking at 180 rpm overnight. For subsequent experiments, the optical density at 600 nm (OD_{600}) was recorded, and a starting OD_{600} of 0.02 was inoculated into fresh LB broth supplemented with carbenicillin (200 $\mu\text{g/ml}$) and incubated at 37°C with shaking at 180 rpm.

Structural modification of HHQ. The synthesis of HHQ, PQS (40, 41), and other HHQ-based analogues (36, 37) was carried out via previously described methods. Novel compounds and compounds that required modified synthesis are described below and in the supplemental material.

TLC analysis. Silica thin-layer chromatographic (TLC) plates, activated by soaking in 5% (wt/vol) K_2HPO_4 for 30 min, were placed in an oven at 100°C for 1 h (42). Analogues (5 μl ; 10 mM) were spotted approximately 1 cm from the bottom. The spots were dried, and the plates were placed in a mobile phase comprising dichloromethane-methanol (95:5). The plate was viewed under UV light when the mobile phase had run 5 cm below the top of the plate.

Biofilm formation, quantification, and visualization. *C. albicans* biofilm formation was carried out in 96-well plates, as previously described (43). Seeding densities for all subsequent experiments ($n = 3$)

were an OD_{600} of 0.05. Biofilm formation was measured as previously described, using a semiquantitative tetrazolium salt, 2,3-bis-(2-methoxy-4-nitro-5-sulfophenyl)-2H tetrazolium-5-carboxanilide inner salt (XTT) reduction assay (44). Experiments were repeated at least three times, with at least eight technical replicates. Visualization of biofilm formation was performed on glass coverslips in 6-well plates using confocal scanning laser microscopy (CSLM). All images were captured using the Zeiss HBO-100 microscope illuminating system, processed using the Zen AIM application imaging program, and converted to JPGs using Axiovision 40 version 4.6.3.0. A minimum of three independent biological repetitions were carried out.

Viable-colony biofilm assay. *C. albicans* biofilms, supplemented with analogues and parent compounds, were grown in 6-well plates and incubated overnight at 37°C . Briefly, the OD_{600} s of *C. albicans* yeast nitrogen base (YNB) cultures were measured, and the cultures were diluted to an OD_{600} of 0.05 in YNB-NP (see below), supplemented with analogues, plated onto 6-well plates, and incubated for 1 h at 37°C . The medium was removed, and the wells were washed twice with sterile phosphate-buffered saline (PBS) and supplemented with fresh YNB-NP with analogues. The plates were incubated overnight at 37°C , after which the medium was removed and the wells were washed with sterile PBS. For serial dilutions, biofilms were harvested by scraping adherent cells into 1 ml PBS, vortexed, and serially diluted in sterile PBS. The serial dilutions (100 μl) were plated onto YPD agar and incubated overnight at 37°C . Colonies were counted and recorded the next day.

***C. albicans* growth curves.** Overnight *C. albicans* cultures grown in YNB were diluted to an OD_{600} of 0.05 in YNB supplemented with analogues. Cultures (200 μl) were added to each well of a 100-well plate and grown for 24-h period on a Bioscreen C spectrophotometer (Growth Curves USA).

RNA isolation and qRT-PCR transcriptional analysis. Overnight *C. albicans* cultures were diluted to an OD_{600} of 0.05 in either YNB or YNB-NP (Difco). The YNB cultures were supplemented with methanol, whereas YNB-NP cultures were supplemented with either 100 μM HHQ or the methanol volume equivalent. The cultures were grown at 37°C with agitation (180 rpm) for 6 h, after which they were centrifuged at 4,000 rpm, the supernatants were discarded, and the pellets were frozen at -20°C until they were processed. RNA was isolated using the MasterPure Yeast RNA purification kit (Cambio Ltd., Cambridge, United Kingdom) according to the manufacturer's specifications and quantified using an ND-1000 spectrophotometer (NanoDrop Technologies, USA). Genomic DNA was enzymatically removed using Turbo DNA-free DNase (Ambion), and samples were confirmed DNA free by PCR. RNA was converted to cDNA using random primers and avian myeloblastosis virus (AMV) reverse transcriptase (Promega) according to the manufacturer's instructions. Quantitative real-time (qRT)-PCR was carried out using the Universal Probe Library (UPL) system (Roche) according to the manufacturer's specifications, and samples were normalized to *C. albicans* actin transcript expression (*ACT1*). A full list of primers and UPL probes used in this study is provided in Table S1 in the supplemental material.

Phenazine extraction. *P. aeruginosa* strains were cultured as described above for 24 h, with the addition of analogues (100 μM), and pyocyanin was extracted as described previously (45). The cultures were centrifuged at 4,000 rpm for 10 min, and the cell-free supernatant (5 ml) was removed. Chloroform (3 ml) was added and mixed by vortexing. After centrifugation at 4,000 rpm for 5 min, the lower aqueous phase was transferred to 0.2 M HCl (2 ml). Samples were mixed by vortexing and centrifuged at 4,000 rpm for 5 min to separate the phases. An aliquot of the top phase (1 ml) was removed and spectrophotometrically analyzed at OD_{570} . Phenazine production was calculated using the following formula: $\text{OD}_{570} \times 2 \times 17.072$, with the units expressed in micrograms per milliliter.

Promoter fusion-based expression analysis. Promoter fusion analyses were performed in a 96-well format, with β -galactosidase activity measured as described previously (46). Briefly, overnight cultures of wild-type PAO1 *pqsA-lacZ* (pLP0996) and mutant strain PAO1 *pqsA* mutant *pqsA*-

lacZ were diluted to an OD₆₀₀ of 0.02 in LB broth. Analogues at 100 μM final concentration were added, mixed, aliquoted into 96-well plates, and incubated overnight at 37°C with shaking. The next day, OD₆₀₀ values were recorded in a plate reader. Aliquots of cells (0.02 ml) were permeabilized (100 mM dibasic sodium phosphate [Na₂HPO₄], 20 mM KCl, 2 mM MgSO₄, 0.8 mg/ml CTAB [hexadecyltrimethylammonium bromide], 0.4 mg/ml sodium deoxycholate, 5.4 μl/ml β-mercaptoethanol) and added to substrate solution (60 mM Na₂HPO₄, 40 mM NaH₂PO₄, 1 mg/ml *o*-nitrophenyl-β-D-galactoside [ONPG], 2.7 μl/ml β-mercaptoethanol). The kinetics of color development was monitored, and the reactions were stopped using 1 M NaCO₃. OD₄₂₀ values were recorded as described above. Miller units were calculated using the following equation; $1,000 \times [(OD_{420}/OD_{600}) \times 0.02 \text{ ml} \times \text{reaction time (min)}]$.

Cytotoxicity assay. Lactate dehydrogenase (LDH) release from a panel of mammalian cells was assayed as a measure of cytotoxicity using an LDH colorimetric kit (Roche) according to the manufacturer's instructions (36). Briefly, IB3-1 lung epithelial cells, A549 human lung adenocarcinoma epithelial cells, DU-145 human prostate cancer cells, and HeLa cervical cancer cells were seeded onto 96-well plates and treated with methanol (control) and analogues. Following 16 h of incubation at 37°C and 5% CO₂, the supernatants were removed and added to a catalyst reaction mixture in a fresh plate and further incubated at 37°C and 5% CO₂ for 30 min to allow color development. After this period, the plate was analyzed on an enzyme-linked immunosorbent assay (ELISA) plate reader at OD₄₉₀. Cytotoxicity was expressed as a percentage of that of cells treated with 0.1% (vol/vol) Triton (100% cytotoxicity).

Statistical analysis. All graphs were compiled using GraphPad Prism (version 5.01) unless otherwise stated. All data were analyzed using built-in GraphPad Prism (version 5.01) functions as specified. The level of significance was set at a *P* value of 0.05, and *post hoc* comparisons between groups were performed using the Bonferroni multiple-comparison test.

RESULTS

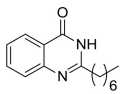
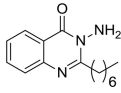
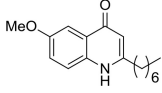
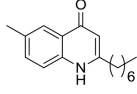
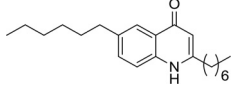
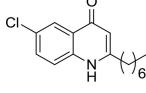
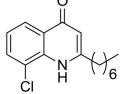
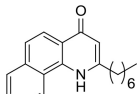
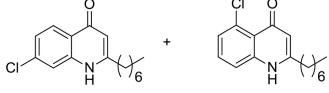
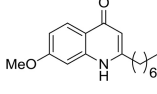
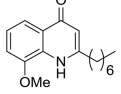
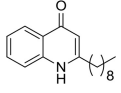
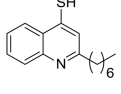
Key modifications of the quinolone framework retain antibiofilm activity toward *C. albicans*. The HHQ molecule has previously been shown to suppress biofilm formation in *C. albicans* at concentrations from 10 to 100 μM (2.47 to 24.7 μg/ml) independent of any effects on the growth of planktonic cells (10). Previous structure-function analysis of the activity of the quinolone framework had implicated the C-3 position as a key component of interspecies antibiofilm activity (36). We undertook further modification of the HHQ parent molecule with the aim of developing viable antibiofilm compounds to target *C. albicans*. These compounds were incorporated into a larger collection of alkylquinolone analogues, systematically modified at different positions on the molecule, and classified on the basis of their substitutions relative to the parent framework HHQ (Table 1).

The suite of analogues was first tested to establish their potency as antibiofilm compounds against *C. albicans* using an optimized XTT assay, a commonly used quantitative method to assess *Candida* biofilm mass and growth (47). As previously described (10), HHQ significantly suppressed biofilm formation compared to untreated and methanol-treated cells, whereas PQS appeared to induce biofilm formation (Fig. 1). When all the analogues were similarly screened by XTT assay, several had antibiofilm activities similar to that of HHQ (compounds 1 and 2 [class I; modified at C-3]; 3, 4, 6, 7, and 9 [class II; modified anthranilate ring]; and 12 [class III; modified alkyl chain]) (Fig. 2a). These analogues were diverse members of classes I, II, and III, suggesting that several components of the HHQ framework contribute to the antibiofilm activity of the parent compound. A number of substitutions led to intermediate antibiofilm activity, including 5, 8, 10, and 11 (class II; modified anthranilate ring) and 15 (class V; modified anthra-

nilate ring and alkyl chain length), while some analogues had completely lost the ability to suppress *C. albicans* biofilm formation, e.g., 13 (class IV; modified C-4) and the class V compounds 14, 16, and 17 (Fig. 2a). While modification of the C-3 position to produce PQS led to loss of antibiofilm activity (Fig. 1), incorporation of an -N-NH₂ moiety (compound 2) at the 3 position or substitution of C-3 with NH (1) did not affect the ability to suppress *C. albicans* biofilm formation (Fig. 2a). Addition of chlorine (Cl) at the C-6 and C-8 positions of the anthranilate ring (compounds 6 and 7) also did not lead to loss of antibiofilm activity. In contrast, the introduction of considerable steric bulk with the addition of an *n*-hexyl alkyl chain at C-6 of the anthranilate ring (compound 5) or elaboration of the aromatic group, as with the naphthyl compound (compound 8), resulted in compounds with significantly less potent antibiofilm activity than HHQ. These data suggest an exquisite level of specificity for the interaction between HHQ and the *C. albicans* biofilm intracellular machinery. Modification of the C-2 alkyl chain from *n*-heptyl (HHQ) to *n*-nonyl C₉ (compound 12) did not affect antibiofilm activity, while parallel modification of the anthranilate ring resulted in a complete loss, as with the class V compound 16 or 17. After modifying the C-4 position (C = O to C = S) (compound 13), the quinolone thiol exhibited an increase in XTT activity (*P* < 0.05) relative to controls (Fig. 2a), comparable to the increase observed in the presence of PQS (Fig. 1). Previously, we have shown that HHQ elicits a dose-dependent reduction in *C. albicans* biofilm formation (10). In order to determine if this also applied to the analogues that retain antibiofilm activity, dose-response analysis of selected compounds, 1, 2, 4, 6, and 12 representing classes I, II, and IV, was undertaken. This revealed compound-specific responses, with 10 μM compounds 2, 4, and 12 being sufficient to elicit a statistically significant reduction in biofilm formation (Fig. 2b). All five compounds reduced biofilm formation when applied at 50 μM and 100 μM. To further confirm the antibiofilm activity of the lead compounds, viable-colony counts were performed on selected analogues using the maximum 100 μM compound dose. This confirmed the outputs from the XTT assays; all the analogues, along with HHQ, significantly reduced viable biofilm cells in comparison to the control (see Fig. S1a in the supplemental material). Importantly, the antibiofilm activity was found to be independent of planktonic growth, which was unaffected in the presence of selected compounds (see Fig. S1b in the supplemental material).

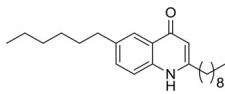
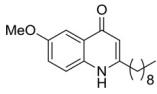
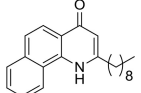
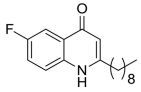
Microscopic staining reveals structural changes in *C. albicans* biofilms. The formation of biofilms in bacteria, yeasts, and fungi is a highly ordered process involving multicellular behavior and has been defined in several stages (22). Confocal microscopy combined with intracellular staining was used to assess the structural integrity and cellular morphology of *C. albicans* incubated on coverslips. Biofilms were individually stained with each of the dyes, and multiple fields of view were visualized to accurately represent the effects of the analogues. The biofilms observed for methanol-treated and untreated controls displayed all the characteristics of a typical *C. albicans* biofilm and were classified as wild type (Fig. 1). Calcofluor, concanavalin A, and FUN-1 staining revealed uniform distribution of chitin/cellulose and cell wall mannosyl/glucosyl residues indicative of viable wild-type morphology (Fig. 1). The analogues identified by XTT assay as causing impaired biofilm formation (1, 2, 3, 4, 6, 7, 9, 12, and 15) exhibited markedly disrupted structures when grown on coverslips and were classified as atypical morphologies (Fig. 3). Cells treated with

TABLE 1 Compound data

Compound	Structure	Yield (%) ^a	MW	R _f ^b	Class ^c
1		76	244.3	0.319	I
2 ^d		3	259.3	0.907	I
3		34	273.4	0.252	II
4		31	257.4	0.286	II
5		35	327.5	0.504	II
6		21	277.8	0.403	II
7		19	277.8	0.630	II
8		46	293.4	0.294	II
9 ^d		6	277.8	0.361	II
10		33	273.4	0.261	II
11		12	273.4	0.504	II
12		23	271.4	0.395	III
13 ^d		48	259.4	1	IV

(Continued on following page)

TABLE 1 (Continued)

Compound	Structure	Yield (%) ^a	MW	R _f ^b	Class ^c
14		16	355.6	0.538	V
15		28	301.4	0.286	V
16		51	321.5	0.462	V
17		16	289.4	0.504	V

^a Yields were isolated over all steps.

^b TLC on silica plates with dichloromethane-MeOH (95:5) mobile phase.

^c Class I, modified C-3; class II, modified anthranilate ring; class III, modified alkyl chain; class IV, modified C-4; class V, modified anthranilate ring and alkyl chain.

^d New compounds synthesized in this study.

class I analogues were found to be largely compromised in their biofilm-forming capabilities and were classified as morphologically atypical. Biofilms produced with both 1 and 2 were significantly distorted, displaying a spindle-like phenotype. Hyphae were short and predominantly displayed yeast cell types rather than hyphal structures. Other structure-disrupting analogues were from classes II, III, and V, suggesting that specific modifications on the anthranilate ring and alkyl chain variation do not significantly affect the antibiofilm activity compared to the parent compound (Fig. 3).

Some analogues, including those that exhibited intermediate activity in the XTT assay, did not alter the biofilm structure, with 5, 11, 13, 14, and 16 all placed into the wild-type morphology group. Biofilms formed in the presence of compound 13 showed

hyperproduction of short hyphae, creating a dense mycelial network (see Fig. S2 in the supplemental material). The remaining analogues from class II, 8 and 10 (see Fig. S1a in the supplemental material), caused significant biofilm disruption, with fragmented hyphae, stunted vegetative growth, and quite large cell debris fields. Cells incubated with the class V molecule 17 induced a severely compromised phenotype (see Fig. S2 in the supplemental material) where debris fields comprising yeast cells and blastospores characterized the structural phenotype.

Enhanced gene transcript expression of *HWP1*, *ECE1*, *ALS3*, *IHD1*, and the uncharacterized open reading frame (ORF) *orf19.2457* provides a molecular mechanism for alkyl quinolone activity toward *C. albicans*. In addition to providing new insights into the interkingdom relationship between these important

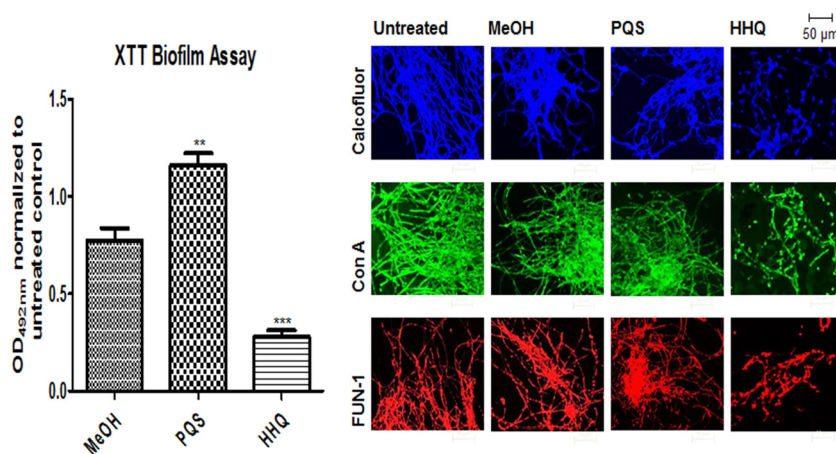


FIG 1 *C. albicans* biofilms are altered in the presence of HHQ. Filamentous *C. albicans* biofilms grown in the presence of PQS and HHQ (100 μM) were assessed structurally by confocal microscopy and metabolically using the XTT biofilm assay. The data (means and standard errors of the mean [SEM]) are representative of three independent biological experiments and are presented relative to the untreated control. A two-tailed paired Student *t* test was performed by comparison of *C. albicans* in the presence of HHQ and PQS with *C. albicans* treated with methanol or ethanol (**, $P \leq 0.01$; ***, $P \leq 0.001$). ConA, concanavalin A.

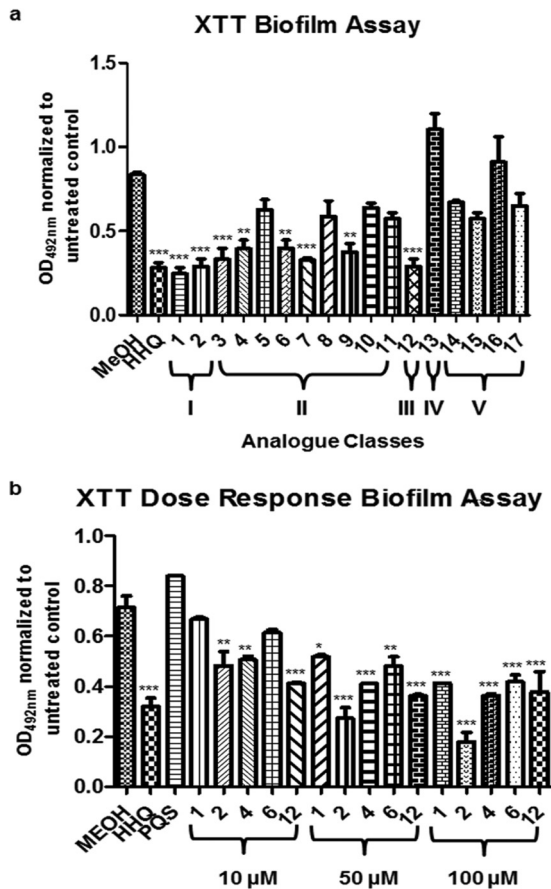


FIG 2 Decoration of HHQ exhibits variable biofilm activity against *C. albicans*. (a) A panel of HHQ-derivatized analogues were incubated with filamentous *C. albicans* and screened for biofilm formation using the metabolic XTT biofilm assay. The data are presented as OD₄₉₂ spectrophotometric output normalized to the untreated control and are representative of at least three independent biological replicates, with error bars representing SEM. (b) Dose-dependent XTT analysis of selected antibiofilm compounds applied at 10, 50, and 100 μ M. The data are the averages from at least two independent biological replicates, each constituting eight technical replicates. Statistical analysis of both data sets was performed by one-way analysis of variance (ANOVA) with Bonferroni corrective testing, and the results are presented relative to the MeOH control values; *, $P \leq 0.05$; **, $P \leq 0.01$; ***, $P \leq 0.001$.

pathogens, strong emphasis has recently been placed on ligand-receptor interactions and the need to provide molecular mechanisms for the action of any potential therapeutic compound (48). We previously implicated *TUP1* in the HHQ-mediated suppression of biofilm formation in *C. albicans*, suggesting a role for the cell wall in this interaction (10, 16). More recently, several reports have shown changes in expression of cell wall-associated genes linked to biofilm formation in the organism (16, 20, 28, 49–51). They included a cohort of eight genes that are proposed to constitute the core filamentous response network, namely, *ALS3*, *ECE1*, *HGT2*, *HWP1*, *IHD1*, *RBT1*, *DCK1*, and the *orf19.2457* gene with unknown function (51). Therefore, transcript expression of a cohort of genes implicated in cell wall biogenesis, hyphal development, biofilm formation, and other related functions that were previously shown to be upregulated during the morphological transition from yeast to filamentous growth was investigated (see Table S1 in the supplemental material) (16, 51). The housekeep-

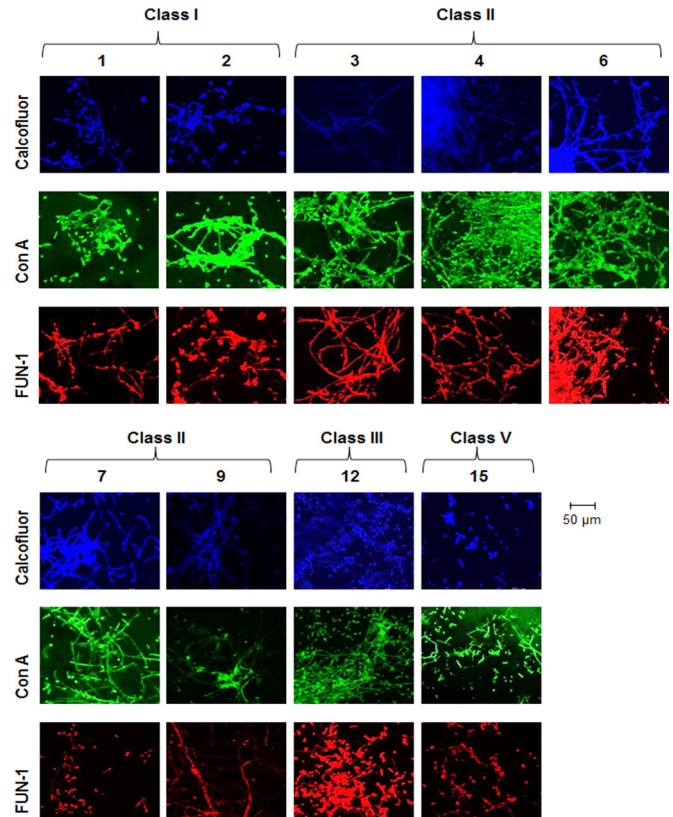


FIG 3 Microscopic analysis reveals altered biofilm structures. Analogues that lead to reduced *C. albicans* biofilm formation in the XTT assay (1, 2, 3, 4, 6, 7, 9, 12, and 15) exhibit compromised biofilm structures. Filamentous *C. albicans* biofilm in the presence of analogues (100 μ M) was stained for chitin and cellulose (calcofluor; blue); lectins that bind to sugars, glycolipids, and glycoproteins (concanavalin A; green); and live/dead cells (FUN-1; red).

ing gene *ACT1* was chosen for normalization based on previous biofilm studies (52). We observed that several transcripts were hyperexpressed in an HHQ-dependent manner, specifically, *HWP1*, *ECE1*, *ALS3*, *IDH1*, and the as yet uncharacterized *orf19.2457* (Fig. 4). The remaining transcripts (*CPH1*, *EFB1*, *ESS1*, *RBT1*, *TUP1*, *BCR1*, *DCK1*, and *HGT2*) yielded expression patterns similar to those of control cells (see Fig. S3 in the supplemental material). It was perhaps somewhat surprising that, while treatment of *C. albicans* with *P. aeruginosa* supernatants has previously been shown to downregulate expression of the *RBT1*, *RBT5*, and *RBT8* genes (16), expression of *RBT1* was unaltered in the presence of HHQ (see Fig. S3 in the supplemental material). Taken together, these data suggest that HHQ induces a specific subset of cell wall proteins in *C. albicans*. Further work is needed to identify the upstream components of this response, although *in silico* screening of *C. albicans* genome sequences has ruled out the presence of an obvious PQS receptor (unpublished data).

Lead compounds display reduced cytotoxic activity toward specific mammalian cell lines. Evaluating the cytotoxicity of synthetic compounds is crucial in the context of developing targeted and highly optimized molecular therapeutics that are benign to human cellular physiology and ideal for use in a clinical environment. In previous work, we showed that analogue 1 was signifi-

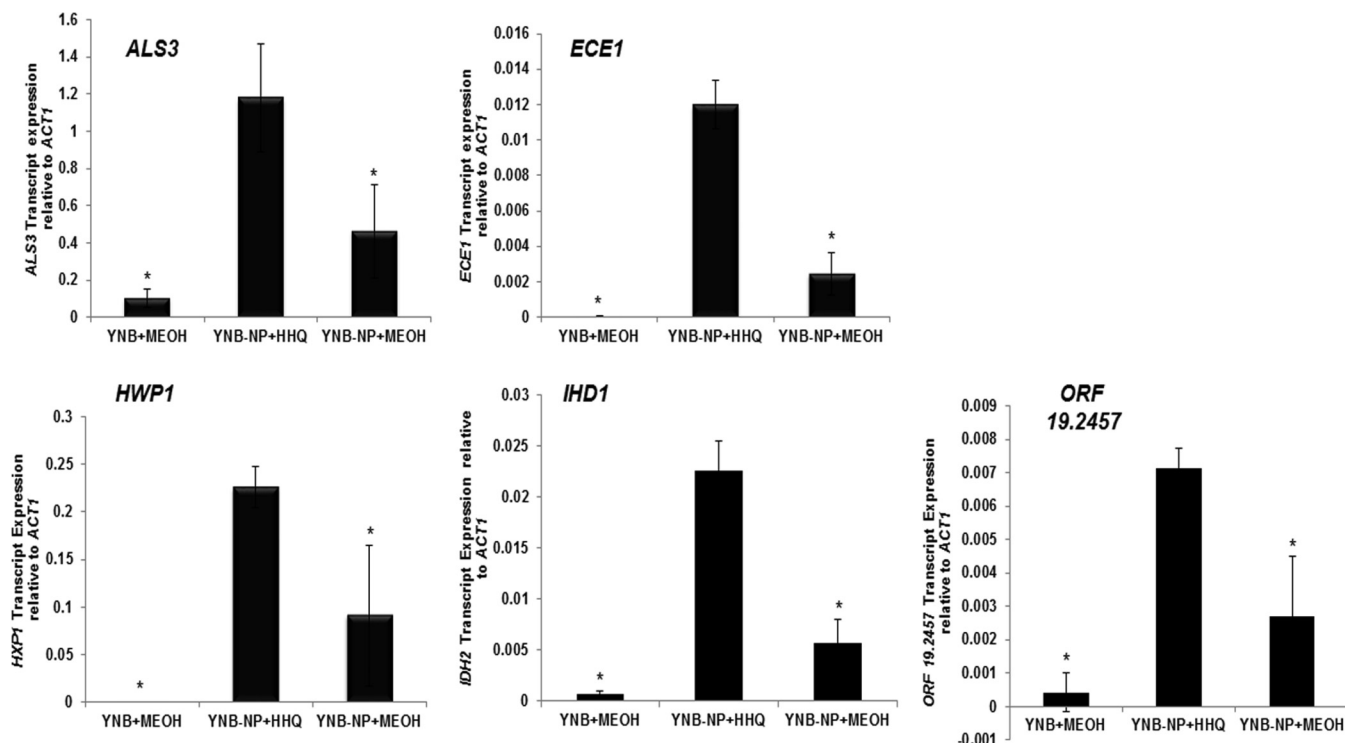


FIG 4 Hyphal pathway genes are hyperexpressed in response to HHQ. Transcript expression analysis (real-time RT-PCR) of a panel of biofilm genes was assessed in *C. albicans* grown in YNB-NP (filament-inducing medium) in 100 μ M HHQ for 6 h at 37°C. All the data were normalized to a housekeeping gene (*ACT1*). The error bars represent standard deviations (SD) of three independent biological replicates. A two-tailed paired Student *t* test was performed by comparison of HHQ-treated cells with methanol control in YNB-NP inducing medium (*, $P \leq 0.05$).

cantly less cytotoxic than HHQ, with an 80% reduction in LDH release relative to the parent compound (36). Therefore, the suite of analogues was tested for *in vitro* cytotoxicity toward IB3-1 airway epithelial cells. Class I analogues exhibited reduced cytotoxicity to IB3-1 cells, with compound 2 displaying approximately 34% toxicity (Fig. 5a). Several class II analogues (4, 6, and 9) exhibited reduced cytotoxicity relative to IB3-1 cells treated with HHQ, with 7 not reaching statistical significance. The class III analogue 12 was comparable to HHQ. Of the analogues that did not retain antibiofilm activity, 5, 8, 10, and 11 exhibited variable cytotoxicity to IB3-1 cells, whereas 13 exhibited considerably reduced cytotoxicity to IB3-1 cells (see Fig. S4 in the supplemental material). Finally, compound 16 exhibited very low levels of cytotoxicity, while 17 was reduced relative to HHQ-treated cells. Compound 15 was the most toxic, killing approximately 91% of all cells (Fig. 5a).

In order to achieve a more comprehensive understanding of the selective toxicity of the lead compounds, several additional cell lines were tested (Fig. 5b). LDH release assays were performed in A549, DU145, and HeLa cell lines in the presence of 100 μ M of the lead compounds and revealed distinct cytotoxicity profiles, with 1 and 9 consistently proving the least cytotoxic of the compounds tested. Compounds 4 and 6 exhibited reduced cytotoxicity in DU145 cells (although not statistically significant) but were comparable to HHQ in both the A549 and HeLa cell lines, while compound 2 exhibited increased cytotoxicity relative to HHQ in DU145 cells (Table 2). These data suggest that cell-specific cytotoxicity analysis will need to be performed prior to the introduction of these compounds in an applied setting.

HHQ analogues display a spectrum of agonist activity toward *P. aeruginosa* virulence. Taken together, compounds 1, 4, 6, and 9 pass both the first and second criteria described above, i.e., they retain antibiofilm activity toward *C. albicans* while exhibiting reduced selective cytotoxicity toward specific host cell lines. However, both HHQ and PQS are coinducers of the virulence-associated LysR-type transcriptional regulator PqsR (41). The structural moieties that underpin the interaction between HHQ/PQS and PqsR remain to be fully characterized, although recent studies have reported diverse classes of PqsR antagonists (53–55) and implicated the hydrophobic pocket situated within the PqsR protein (56). Therefore, in order to assess whether the lead compounds could elicit a virulence response from *P. aeruginosa*, phenazine production and *pqsA* promoter activity (57) were monitored in a *pqsA* mutant where the capacity to produce native HHQ and PQS had been lost.

Both HHQ and PQS restored phenazine production in the *pqsA* mutant strain (Fig. 6a). In contrast, the majority of analogues did not restore phenazine production in the strain, with the notable exception of compound 9. Several analogues from different classes did partially restore phenazine production in the mutant background, including compounds 10, 12, and 17 (Fig. 6; see Fig. S5 in the supplemental material). None of the analogues interfered with phenazine production in the wild-type PAO1 strain, suggesting that they are ineffective as PQS antagonists (see Fig. S5 in the supplemental material).

Similarly, while some degree of PqsR agonist activity was observed in the presence of compounds 6, 9, 10, 12, 13, and 17, only HHQ and PQS significantly induced promoter activity. All the

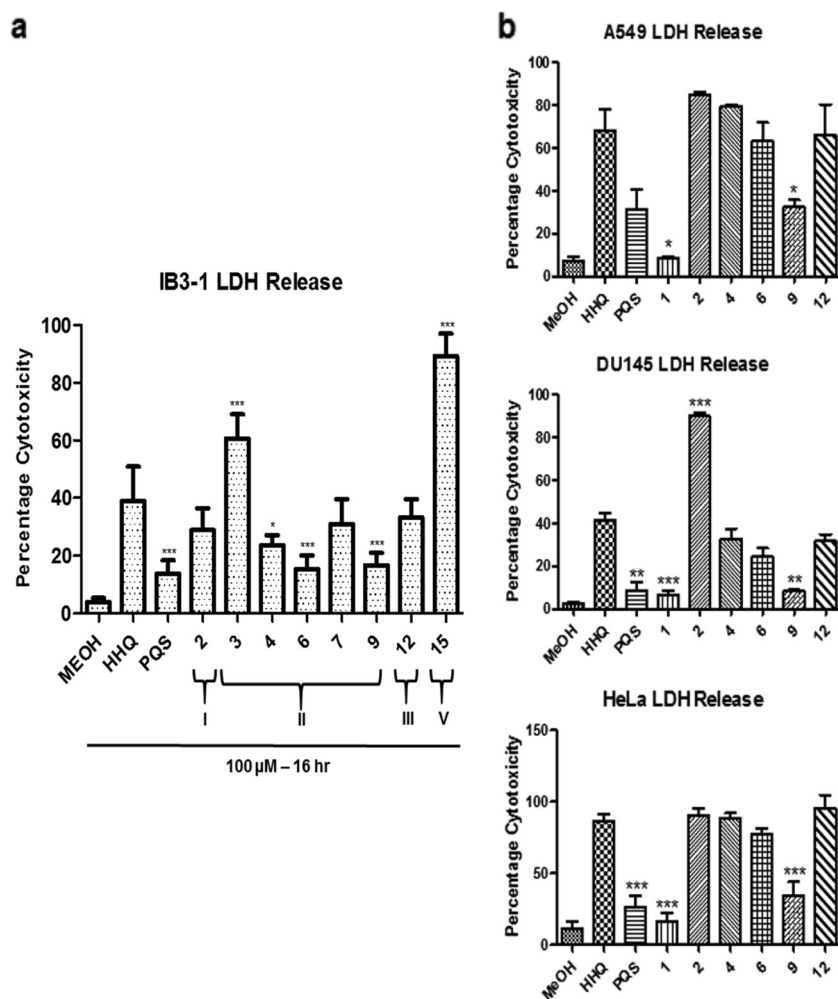


FIG 5 Cytotoxicity toward specific mammalian cell lines is reduced in lead compounds. (a) Cytotoxicity, measured as a percentage of total LDH released from IB3-1 cells treated with 0.1% Triton X-100 (100% cytotoxicity), was significantly reduced in the presence of several lead compounds. The data (means and SEM) are representative of three independent biological experiments. (b) Selected lead compounds were tested against A549, DU145, and HeLa cell lines. The data represent four independent biological replicates, and all the data points are normalized to Triton X-100 as described for panel a. One-way ANOVA was performed, with Bonferroni corrective testing on all data sets, and comparison to an MeOH control is presented; *, $P \leq 0.05$; **, $P \leq 0.01$; ***, $P \leq 0.001$.

other analogues did not influence promoter activity in this system (Fig. 6B; see Fig. S5 in the supplemental material). Somewhat surprisingly, antagonistic activity toward *pqsA* promoter activity was not observed, with almost all the analogues failing to significantly suppress *pqsA* promoter activity in the wild-type strain (see Fig. S5 in the supplemental material). The relative ineffectiveness of these

analogues as PQS antagonists may in part be due to hydroxylation of HHQ analogues (H at C-3) to PQS analogues (OH at C-3), thus establishing the nonantagonistic behavior explained by a recent report by Lu and colleagues, where the action of PqsH rendered anti-PQS compounds ineffective through bioconversion (55).

DISCUSSION

Current antimicrobial therapies tend to be non-pathogen specific, and there is evidence to suggest that the availability of relatively nontoxic broad-spectrum therapies has contributed to the emergence of resistance among both targeted and nontargeted microbes (58, 59). Consequently, there is an urgent need to create innovative new options for the targeted prevention of microbial infection while avoiding the inevitable emergence of resistance that is the hallmark of broad-spectrum antibiotic therapies (59, 60). Increasingly, industry, academia, and regulatory bodies have become interested in single-pathogen therapies to treat highly resistant or totally resistant bacterial pathogens, rightly viewed as an area of high unmet need (61–63). Exploiting interkingdom com-

TABLE 2 Selective toxicity indices of lead compounds

Compound	Selective toxicity index (% toxicity)			
	IB3-1	A549	DU145	HeLa
HHQ	26–50	51–75	26–50	76–100
PQS	0–25	26–50	0–25	0–25
1	0–25	0–25	0–25	0–25
2	26–50	76–100	76–100	76–100
4	0–25	76–100	26–50	76–100
6	26–50	51–75	0–25	76–100
9	0–25	26–50	0–25	26–50
12	26–50	51–75	26–50	76–100

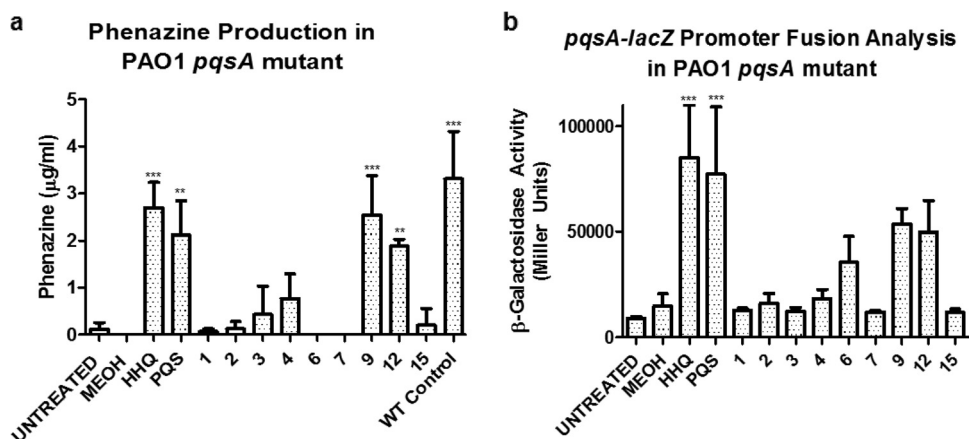


FIG 6 Influence of HHQ analogues on PQS-dependent virulence phenotypes in *P. aeruginosa*. Phenazine production (a) and *pqsA-lacZ* promoter activity (b) were quantified in a PAO1 *pqsA* mutant in the presence of HHQ, PQS, and lead compounds. The data are presented as means and SEM and are representative of at least three independent biological replicates. One-way ANOVA was performed, with Bonferroni corrective testing, and statistical significance relative to the MeOH control is presented; **, $P \leq 0.01$; ***, $P \leq 0.001$.

munication networks, and the mode of action of the chemical messages or signals employed therein, offers us a powerful platform from which to meet this need.

Previously, we showed that the HHQ interkingdom signal molecule from *P. aeruginosa* could suppress biofilm formation in *C. albicans* at concentrations ranging from 10 to 100 μM (2.47 to 24.7 $\mu\text{g/ml}$) (10). This suppression occurred independently of any growth limitation in planktonic cells, and morphogenesis on spider medium was also found to be unaffected (10). The design and subsequent analysis of a suite of analogues based on the core HHQ quinolone framework has led to the identification of several lead compounds that retain antibiofilm activity toward *C. albicans* but exhibit significantly reduced cytotoxicity toward IB3-1 epithelial cells compared with the parent HHQ molecule. The selective cytotoxicities of the lead compounds, together with the dose-dependent antibiofilm effects, will be key considerations in determining the cell line-specific therapeutic index of lead analogues as part of the ongoing development of these compounds. Furthermore, unlike HHQ, these lead compounds are now inactive toward the *P. aeruginosa* PqsR quorum-sensing system, a critical requirement for their potential future development as antibiofilm therapeutics. In addition, the ability to generate hydrochloride salts of the compounds (reference 36 and data not shown) suggests that the solubility of future therapeutics based on these scaffolds will not be a bottleneck. Several strategies have been proposed for the implementation of antibiofilm compounds as clinical therapeutics to target *C. albicans* biofilm infections (64). As the HHQ analogues possess antibiofilm, but not anti-*Candida*, activity, they would disrupt the formation of biofilms but not likely remove the planktonic cells that remain at the site of infection. Therefore, combination with conventional antifungal compounds would be required for effective clearance. Alternatively, where the potency of the antibiofilm activity can be synthetically enhanced through further derivatization, clearance by the immune system might also be realistic.

The molecular mechanisms through which AHQs and the lead compounds identified in this study disrupt the formation of biofilms by *C. albicans* remain to be fully elucidated. Previ-

ously, we have shown that HHQ does not affect adhesion, but rather directly impacts the subsequent developmental stages in a TUP1-dependent manner (10). In this study, we have shown that the expression of several cell wall-associated genes is increased in response to HHQ during the switch to hyphal growth. These genes have previously been implicated in the formation of *C. albicans* biofilms and have been shown to exhibit increased levels of expression during the hyphal transition (50, 51, 65). Therefore, antibiofilm compounds might be expected to suppress this induction rather than enhance it. However, five of the target genes tested exhibited an increase in expression relative to control cells under inducing conditions. This may be a reflection of the previous observation that HHQ interferes with the later stages of biofilm development (10). Alternatively, this hyperexpression phenotype may affect the capacity of the cell to engineer a community-based biofilm. Future studies will focus on elucidating the pathways through which *C. albicans* perceives and responds to challenge with HHQ with the aim of identifying potential therapeutic targets.

Further work using defined *in vivo* models of biofilms and infection will be required to further the development and evaluation of these small molecules as antibiofilm compounds. Models are now available for the investigation of infections involving medical devices, such as vascular catheters, dentures, urinary catheters, and subcutaneous implants, as well as mucosal biofilm infections (66). The ongoing development of cell-based or animal models to study *in vivo* infections (66–69), whether as single-pathogen or coculture systems (70), has provided a well-equipped tool kit for the preclinical assessment of these AHQ-based compounds.

Conclusions. In this study, we have functionalized the important microbial signaling molecules HHQ and PQS in order to exploit their interkingdom roles in controlling biofilm formation in *C. albicans*. In addition to deciphering further insights into the molecular mechanism through which these chemical messages elicit a biofilm-suppressive response from *C. albicans*, the bioactivity of several lead compounds has provided a viable platform for the development of next-generation therapeutics. Crucially, some of these compounds are nontoxic to mammalian cells and

have been rendered incapable of activating *P. aeruginosa* virulence systems, thus highlighting their potential utility as an effective therapy combatting human infection.

ACKNOWLEDGMENTS

F.J.R., G.P.M., and F.O. conceived and designed the investigation. F.J.R., J.P.P., L.G., and D.F.W. performed the biological experimentation, while R.C., R.M.S., and E.O.M. conducted the chemical synthesis. F.J.R., J.P.P., and F.O. wrote the manuscript, and we all read and edited the final draft.

FUNDING INFORMATION

This work, including the efforts of Gerard P. McGlacken, was funded by Science Foundation Ireland (SFI) (SFI/12/RC/2275). This work, including the efforts of Fergal O’Gara, was funded by Science Foundation Ireland (SFI) (SSPC-2 12/RC/2275, 13/TIDA/B2625, 12/TIDA/B2411, 12/TIDA/B2405, and 14/TIDA/2438). This work, including the efforts of Fergal O’Gara, was funded by European Commission (EC) (FP7-PEOPLE-2013-ITN 607786, FP7-KBBE-2012-6 CP-TP-312184, FP7-KBBE-2012-6 311975, OCEAN 2011-2 287589, Marie Curie 256596, and EU-634486). This work, including the efforts of Fergal O’Gara, was funded by Health Research Board (HRB) (Irish Thoracic Society MRCG-2014-6). This work, including the efforts of Fergal O’Gara, was funded by Teagasc (Walsh Fellowship 2013). This work, including the efforts of Fergal O’Gara, was funded by Department of Agriculture, Food and the Marine (FIRM/RSE/CoFoRD, FIRM 08/RDC/629, FIRM 1/F009/MabS, and FIRM 13/F/516). This work, including the efforts of Fergal O’Gara, was funded by Irish Research Council for Science, Engineering and Technology (IRCSET) (PD/2011/2414 and GOIPG/2014/647). This work, including the efforts of Fergal O’Gara, was funded by Marine Institute (Foras Na Mara) (Beaufort award C2CRA 2007/082).

G.P.M. thanks the Irish Research Council (R.M.S. and R.C.) and the UCC Strategic Research Fund (E.O.M.). The funders had no role in study design, data collection and interpretation, or the decision to submit the work for publication.

REFERENCES

- Cooper MA, Shlaes D. 2011. Fix the antibiotics pipeline. *Nature* 472:32. <http://dx.doi.org/10.1038/472032a>.
- European Centre for Disease Prevention and Control and European Medicines Agency. 2009. The bacterial challenge: time to react. European Centre for Disease Prevention and Control and European Medicines Agency, Stockholm, Sweden.
- Spellberg B, Powers JH, Brass EP, Miller LG, Edwards JE, Jr. 2004. Trends in antimicrobial drug development: implications for the future. *Clin Infect Dis* 38:1279–1286. <http://dx.doi.org/10.1086/420937>.
- Bjarnsholt T, Ciofu O, Molin S, Givskov M, Hoiby N. 2013. Applying insights from biofilm biology to drug development; can a new approach be developed? *Nat Rev Drug Discov* 12:791–808. <http://dx.doi.org/10.1038/nrd4000>.
- Davies D. 2003. Understanding biofilm resistance to antibacterial agents. *Nat Rev Drug Discov* 2:114–122. <http://dx.doi.org/10.1038/nrd1008>.
- Dong YH, Wang LH, Xu JL, Zhang HB, Zhang XF, Zhang LH. 2001. Quenching quorum-sensing-dependent bacterial infection by an N-acyl homoserine lactonase. *Nature* 411:813–817. <http://dx.doi.org/10.1038/35081101>.
- Fux CA, Costerton JW, Stewart PS, Stoodley P. 2005. Survival strategies of infectious biofilms. *Trends Microbiol* 13:34–40. <http://dx.doi.org/10.1016/j.tim.2004.11.010>.
- Hoiby N, Ciofu O, Johansen HK, Song ZJ, Moser C, Jensen PO, Molin S, Givskov M, Tolker-Nielsen T, Bjarnsholt T. 2011. The clinical impact of bacterial biofilms. *Int J Oral Sci* 3:55–65. <http://dx.doi.org/10.4248/IJOS11026>.
- Rasmussen TB, Givskov M. 2006. Quorum sensing inhibitors: a bargain of effects. *Microbiology* 152:895–904. <http://dx.doi.org/10.1099/mic.0.28601-0>.
- Reen FJ, Mooij MJ, Holcombe LJ, McSweeney CM, McGlacken GP, Morrissey JP, O’Gara F. 2011. The *Pseudomonas* quinolone signal (PQS), and its precursor HHQ, modulate interspecies and interkingdom behaviour. *FEMS Microbiol Ecol* 77:413–428. <http://dx.doi.org/10.1111/j.1574-6941.2011.01121.x>.
- Rutherford ST, Bassler BL. 2012. Bacterial quorum sensing: its role in virulence and possibilities for its control. *Cold Spring Harb Perspect Med* 2:a012427. <http://dx.doi.org/10.1101/cshperspect.a012427>.
- Ternent L, Dyson RJ, Krachler AM, Jabbari S. 2015. Bacterial fitness shapes the population dynamics of antibiotic-resistant and -susceptible bacteria in a model of combined antibiotic and anti-virulence treatment. *J Theor Biol* 372:1–11. <http://dx.doi.org/10.1016/j.jtbi.2015.02.011>.
- Cox CE, McClelland M, Teplitski M. 2013. Consequences of disrupting *Salmonella* AI-2 signaling on interactions within soft rots. *Phytopathology* 103:352–361. <http://dx.doi.org/10.1094/PHYTO-09-12-0237-FI>.
- Dong YH, Gusti AR, Zhang Q, Xu JL, Zhang LH. 2002. Identification of quorum-quenching N-acyl homoserine lactonases from *Bacillus* species. *Appl Environ Microbiol* 68:1754–1759. <http://dx.doi.org/10.1128/AEM.68.4.1754-1759.2002>.
- Hentzer M, Riedel K, Rasmussen TB, Heydorn A, Andersen JB, Parsek MR, Rice SA, Eberl L, Molin S, Hoiby N, Kjelleberg S, Givskov M. 2002. Inhibition of quorum sensing in *Pseudomonas aeruginosa* biofilm bacteria by a halogenated furanone compound. *Microbiology* 148:87–102. <http://dx.doi.org/10.1099/00221287-148-1-87>.
- Holcombe LJ, McAlester G, Munro CA, Enjalbert B, Brown AJ, Gow NA, Ding C, Butler G, O’Gara F, Morrissey JP. 2010. *Pseudomonas aeruginosa* secreted factors impair biofilm development in *Candida albicans*. *Microbiology* 156:1476–1486. <http://dx.doi.org/10.1099/mic.0.037549-0>.
- Janssens JC, Steenackers H, Robijns S, Gellens E, Levin J, Zhao H, Hermans K, De Coster D, Verhoeven TL, Marchal K, Vanderleyden J, De Vos DE, De Keersmaecker SC. 2008. Brominated furanones inhibit biofilm formation by *Salmonella enterica* serovar Typhimurium. *Appl Environ Microbiol* 74:6639–6648. <http://dx.doi.org/10.1128/AEM.01262-08>.
- O’Loughlin CT, Miller LC, Siryaporn A, Drescher K, Semmelhack MF, Bassler BL. 2013. A quorum-sensing inhibitor blocks *Pseudomonas aeruginosa* virulence and biofilm formation. *Proc Natl Acad Sci U S A* 110:17981–17986. <http://dx.doi.org/10.1073/pnas.1316981110>.
- Zambelloni R, Marquez R, Roe AJ. 2015. Development of antivirulence compounds: a biochemical review. *Chem Biol Drug Des* 85:43–55. <http://dx.doi.org/10.1111/cbdd.12430>.
- Desai JV, Mitchell AP, Andes DR. 2014. Fungal biofilms, drug resistance, and recurrent infection. *Cold Spring Harb Perspect Med* 4:a019729. <http://dx.doi.org/10.1101/cshperspect.a019729>.
- Perlroth J, Choi B, Spellberg B. 2007. Nosocomial fungal infections: epidemiology, diagnosis, and treatment. *Med Mycol* 45:321–346. <http://dx.doi.org/10.1080/13693780701218689>.
- Ramage G, Rajendran R, Sherry L, Williams C. 2012. Fungal biofilm resistance. *Int J Microbiol* 2012:528521. <http://dx.doi.org/10.1155/2012/528521>.
- Feldman M, Shenderovich J, Al-Quntar AA, Friedman M, Steinberg D. 2015. Sustained release of a novel anti-quorum-sensing agent against oral fungal biofilms. *Antimicrob Agents Chemother* 59:2265–2272. <http://dx.doi.org/10.1128/AAC.04212-14>.
- Moudgal V, Sobel J. 2010. Antifungals to treat *Candida albicans*. *Expert Opin Pharmacother* 11:2037–2048. <http://dx.doi.org/10.1517/14656566.2010.493875>.
- Chandra J, Mukherjee P, Ghannoum A. 2012. *Candida* biofilms associated with CVC and medical devices. *Mycoses* 55:46–57. <http://dx.doi.org/10.1111/j.1439-0507.2011.02149.x>.
- Lynch AS, Robertson GT. 2008. Bacterial and fungal biofilm infections. *Annu Rev Med* 59:415–428. <http://dx.doi.org/10.1146/annurev.med.59.110106.132000>.
- Bink A, Pellens K, Cammue BPA, Thevissen K. 2011. Anti-biofilm strategies: how to eradicate *Candida* biofilms. *Open Mycol J* 5:29–38. <http://dx.doi.org/10.2174/1874437001105010029>.
- Finkel JS, Xu W, Huang D, Hill EM, Desai JV, Woolford CA, Nett JE, Taff H, Norice CT, Andes DR, Lanni F, Mitchell AP. 2012. Portrait of *Candida albicans* adherence regulators. *PLoS Pathog* 8:e1002525. <http://dx.doi.org/10.1371/journal.ppat.1002525>.
- Miceli MH, Bernardo SM, Lee SA. 2009. *In vitro* analyses of the combination of high-dose doxycycline and antifungal agents against *Candida*

- albicans* biofilms. *Int J Antimicrob Agents* 34:326–332. <http://dx.doi.org/10.1016/j.ijantimicag.2009.04.011>.
30. Bose S, Ghosh AK. 2011. Biofilms: a challenge to medical science. *J Clin Diagn Res* 5:127–130.
 31. Peleg AY, Hogan DA, Mylonakis E. 2010. Medically important bacterial-fungal interactions. *Nat Rev Microbiol* 8:340–349. <http://dx.doi.org/10.1038/nrmicro2313>.
 32. Wargo MJ, Hogan DA. 2006. Fungal-bacterial interactions: a mixed bag of mingling microbes. *Curr Opin Microbiol* 9:359–364. <http://dx.doi.org/10.1016/j.mib.2006.06.001>.
 33. Cugini C, Morales DK, Hogan DA. 2010. *Candida albicans*-produced farnesol stimulates *Pseudomonas* quinolone signal production in LasR-defective *Pseudomonas aeruginosa* strains. *Microbiology* 156:3096–3107. <http://dx.doi.org/10.1099/mic.0.037911-0>.
 34. Hodgkinson JT, Galloway WR, Saraf S, Baxendale IR, Ley SV, Ladlow M, Welch M, Spring DR. 2011. Microwave and flow syntheses of *Pseudomonas* quinolone signal (PQS) and analogues. *Org Biomol Chem* 9:57–61. <http://dx.doi.org/10.1039/C0OB00652A>.
 35. Mashburn-Warren L, Howe J, Brandenburg K, Whiteley M. 2009. Structural requirements of the *Pseudomonas* quinolone signal for membrane vesicle stimulation. *J Bacteriol* 191:3411–3414. <http://dx.doi.org/10.1128/JB.00052-09>.
 36. Reen FJ, Clarke SL, Legendre C, McSweeney CM, Eccles KS, Lawrence SE, O'Gara F, McGlacken GP. 2012. Structure-function analysis of the C-3 position in analogues of microbial behavioural modulators HHQ and PQS. *Org Biomol Chem* 10:8903–8910. <http://dx.doi.org/10.1039/c2ob26823j>.
 37. Reen FJ, Shanahan R, Cano R, O'Gara F, McGlacken GP. 2015. A structure activity-relationship study of the bacterial signal molecule HHQ reveals swarming motility inhibition in *Bacillus atrophaeus*. *Org Biomol Chem* 13:5537–5541. <http://dx.doi.org/10.1039/C5OB00315F>.
 38. Deziel E, Lepine F, Milot S, He J, Mindrinos MN, Tompkins RG, Rahme LG. 2004. Analysis of *Pseudomonas aeruginosa* 4-hydroxy-2-alkylquinolines (HAQs) reveals a role for 4-hydroxy-2-heptylquinoline in cell-to-cell communication. *Proc Natl Acad Sci U S A* 101:1339–1344. <http://dx.doi.org/10.1073/pnas.0307694100>.
 39. Diggle SP, Matthijs S, Wright VJ, Fletcher MP, Chhabra SR, Lamont IL, Kong X, Hider RC, Cornelis P, Camara M, Williams P. 2007. The *Pseudomonas aeruginosa* 4-quinolone signal molecules HHQ and PQS play multifunctional roles in quorum sensing and iron entrapment. *Chem Biol* 14:87–96. <http://dx.doi.org/10.1016/j.chembiol.2006.11.014>.
 40. McGlacken GP, McSweeney CM, O'Brien T, Lawrence SE, Elcoate CJ, Reen FJ, O'Gara F. 2010. Synthesis of 3-halo-analogues of HHQ, subsequent cross-coupling and first crystal structure of *Pseudomonas* quinolone signal (PQS). *Tetrahedron Lett* 51:5919–5921. <http://dx.doi.org/10.1016/j.tetlet.2010.09.013>.
 41. Pesci EC, Milbank JB, Pearson JP, McKnight S, Kende AS, Greenberg EP, Iglewski BH. 1999. Quinolone signaling in the cell-to-cell communication system of *Pseudomonas aeruginosa*. *Proc Natl Acad Sci U S A* 96:11229–11234. <http://dx.doi.org/10.1073/pnas.96.20.11229>.
 42. Fletcher MP, Diggle SP, Camara M, Williams P. 2007. Biosensor-based assays for PQS, HHQ and related 2-alkyl-4-quinolone quorum sensing signal molecules. *Nat Protoc* 2:1254–1262. <http://dx.doi.org/10.1038/nprot.2007.158>.
 43. Ramage G, Vande Walle K, Wickes BL, Lopez-Ribot JL. 2001. Standardized method for in vitro antifungal susceptibility testing of *Candida albicans* biofilms. *Antimicrob Agents Chemother* 45:2475–2479. <http://dx.doi.org/10.1128/AAC.45.9.2475-2479.2001>.
 44. Hawser S. 1996. Comparisons of the susceptibilities of planktonic and adherent *Candida albicans* to antifungal agents: a modified XTT tetrazolium assay using synchronised C-albicans cells. *J Med Vet Mycol* 34:149–152. <http://dx.doi.org/10.1080/02681219680000231>.
 45. Essar DW, Eberly L, Hadero A, Crawford IP. 1990. Identification and characterization of genes for a second anthranilate synthase in *Pseudomonas aeruginosa*: interchangeability of the two anthranilate synthases and evolutionary implications. *J Bacteriol* 172:884–900.
 46. Miller JH. 1972. Experiments in molecular genetics. Cold Spring Harbor Laboratory Press, Cold Spring Harbor, NY.
 47. Nett JE, Cain MT, Crawford K, Andes DR. 2011. Optimizing a *Candida* biofilm microtiter plate model for measurement of antifungal susceptibility by tetrazolium salt assay. *J Clin Microbiol* 49:1426–1433. <http://dx.doi.org/10.1128/JCM.02273-10>.
 48. Baell J, Walters MA. 2014. Chemistry: chemical con artists foil drug discovery. *Nature* 513:481–483. <http://dx.doi.org/10.1038/513481a>.
 49. Bandara HM, Cheung BP, Watt RM, Jin LJ, Samaranyake LP. 2013. Secretory products of *Escherichia coli* biofilm modulate *Candida* biofilm formation and hyphal development. *J Invest Clin Dent* 4:186–199. <http://dx.doi.org/10.1111/jicd.12048>.
 50. Finkel JS, Mitchell AP. 2011. Genetic control of *Candida albicans* biofilm development. *Nat Rev Microbiol* 9:109–118. <http://dx.doi.org/10.1038/nrmicro2475>.
 51. Martin R, Albrecht-Eckardt D, Brunke S, Hube B, Hunniger K, Kurzai O. 2013. A core filamentation response network in *Candida albicans* is restricted to eight genes. *PLoS One* 8:e58613. <http://dx.doi.org/10.1371/journal.pone.0058613>.
 52. Nailis H, Coenye T, Van Nieuwerburgh F, Deforce D, Nelis HJ. 2006. Development and evaluation of different normalization strategies for gene expression studies in *Candida albicans* biofilms by real-time PCR. *BMC Mol Biol* 7:25. <http://dx.doi.org/10.1186/1471-2199-7-25>.
 53. Klein T, Henn C, de Jong JC, Zimmer C, Kirsch B, Maurer CK, Pistorius D, Muller R, Steinbach A, Hartmann RW. 2012. Identification of small-molecule antagonists of the *Pseudomonas aeruginosa* transcriptional regulator PqsR: biophysically guided hit discovery and optimization. *ACS Chem Biol* 7:1496–1501. <http://dx.doi.org/10.1021/cb300208g>.
 54. Lu C, Kirsch B, Zimmer C, de Jong JC, Henn C, Maurer CK, Musken M, Haussler S, Steinbach A, Hartmann RW. 2012. Discovery of antagonists of PqsR, a key player in 2-alkyl-4-quinolone-dependent quorum sensing in *Pseudomonas aeruginosa*. *Chem Biol* 19:381–390. <http://dx.doi.org/10.1016/j.chembiol.2012.01.015>.
 55. Lu C, Maurer CK, Kirsch B, Steinbach A, Hartmann RW. 2014. Overcoming the unexpected functional inversion of a PqsR antagonist in *Pseudomonas aeruginosa*: an in vivo potent antivirulence agent targeting pqs quorum sensing. *Angew Chem Int Ed Engl* 53:1109–1112. <http://dx.doi.org/10.1002/anie.201307547>.
 56. Ilangovan A, Fletcher M, Rampioni G, Pustelny C, Rumbaugh K, Heeb S, Camara M, Truman A, Chhabra SR, Emsley J, Williams P. 2013. Structural basis for native agonist and synthetic inhibitor recognition by the *Pseudomonas aeruginosa* quorum sensing regulator PqsR (MvFR). *PLoS Pathog* 9:e1003508. <http://dx.doi.org/10.1371/journal.ppat.1003508>.
 57. McGrath S, Wade DS, Pesci EC. 2004. Dueling quorum sensing systems in *Pseudomonas aeruginosa* control the production of the *Pseudomonas* quinolone signal (PQS). *FEMS Microbiol Lett* 230:27–34. [http://dx.doi.org/10.1016/S0378-1097\(03\)00849-8](http://dx.doi.org/10.1016/S0378-1097(03)00849-8).
 58. Casadevall A. 1996. Crisis in infectious diseases: time for a new paradigm? *Clin Infect Dis* 23:790–794. <http://dx.doi.org/10.1093/clinids/23.4.790>.
 59. Casadevall A. 2009. The case for pathogen-specific therapy. *Expert Opin Pharmacother* 10:1699–1703. <http://dx.doi.org/10.1517/14656560903066837>.
 60. Spellberg B, Rex JH. 2013. The value of single-pathogen antibacterial agents. *Nat Rev Drug Discov* 12:963. <http://dx.doi.org/10.1038/nrd3957-cl>.
 61. European Medicines Agency. 2012. Addendum to the note for guidance on evaluation of medicinal products indicated for treatment of bacterial infections (CPMP/EWP/558/95 REV 2) to address indication-specific clinical data. European Medicines Agency, London, United Kingdom.
 62. Alemayehu D, Quinn J, Cook J, Kunkel M, Knirsch CA. 2012. A paradigm shift in drug development for treatment of rare multidrug-resistant gram-negative pathogens. *Clin Infect Dis* 55:562–567. <http://dx.doi.org/10.1093/cid/cis503>.
 63. Infectious Diseases Society of America. 2012. White paper: recommendations on the conduct of superiority and organism-specific clinical trials of antibacterial agents for the treatment of infections caused by drug-resistant bacterial pathogens. *Clin Infect Dis* 55:1031–1046. <http://dx.doi.org/10.1093/cid/cis688>.
 64. Nett JE. 2014. Future directions for anti-biofilm therapeutics targeting *Candida*. *Expert Rev Anti Infect Ther* 12:375–382. <http://dx.doi.org/10.1586/14787210.2014.885838>.
 65. Desai JV, Mitchell AP. 2015. *Candida albicans* biofilm development and its genetic control. *Microbiol Spectr* 3. <http://dx.doi.org/10.1128/microbiolspec.MB-0005-2014>.
 66. Nett JE, Andes DR. 2015. Fungal biofilms: in vivo models for discovery of anti-biofilm drugs. *Microbiol Spectr* 3. <http://dx.doi.org/10.1128/microbiolspec.MB-0008-2014>.
 67. Chauhan A, Bernardin A, Mussard W, Kriegel I, Esteve M, Ghigo

- JM, Beloin C, Semetey V. 2014. Preventing biofilm formation and associated occlusion by biomimetic glycocalyxlike polymer in central venous catheters. *J Infect Dis* 210:1347–1356. <http://dx.doi.org/10.1093/infdis/jiu249>.
68. Chauhan A, Ghigo JM, Beloin C. 2016. Study of in vivo catheter biofilm infections using pediatric central venous catheter implanted in rat. *Nat Protoc* 11:525–541. <http://dx.doi.org/10.1038/nprot.2016.033>.
69. Kucharikova S, Neirinck B, Sharma N, Vleugels J, Lagrou K, Van Dijck P. 2015. *In vivo Candida glabrata* biofilm development on foreign bodies in a rat subcutaneous model. *J Antimicrob Chemother* 70:846–856. <http://dx.doi.org/10.1093/jac/dku447>.
70. Sobue T, Diaz P, Xu H, Bertolini M, Dongari-Bagtzoglou A. 2016. Experimental models of *C. albicans*-streptococcal coinfection. *Methods Mol Biol* 1356:137–152. http://dx.doi.org/10.1007/978-1-4939-3052-4_10.